

AFFTC-PA-11139



SPACE-TIME CODING FOR AERONAUTICAL TELEMETRY: PART II – EXPERIMENTAL RESULTS

**KIP TEMPLE
AIR FORCE FLIGHT TEST CENTER
EDWARDS AFB, CA**

**MICHAEL RICE
BRIGHAM YOUNG UNIVERSITY
PROVO, UT**

10 JUNE 2011

Approved for public release A: distribution is unlimited.

**AIR FORCE FLIGHT TEST CENTER
EDWARDS AIR FORCE BASE, CALIFORNIA
AIR FORCE MATERIEL COMMAND
UNITED STATES AIR FORCE**

**A
F
F
T
C**

REPORT DOCUMENTATION PAGE				Form Approved OMB No. 0704-0188	
Public reporting burden for this collection of information is estimated to average 1 hour per response, including the time for reviewing instructions, searching existing data sources, gathering and maintaining the data needed, and completing and reviewing this collection of information. Send comments regarding this burden estimate or any other aspect of this collection of information, including suggestions for reducing this burden to Department of Defense, Washington Headquarters Services, Directorate for Information Operations and Reports (0704-0188), 1215 Jefferson Davis Highway, Suite 1204, Arlington, VA 22202-4302. Respondents should be aware that notwithstanding any other provision of law, no person shall be subject to any penalty for failing to comply with a collection of information if it does not display a currently valid OMB control number. PLEASE DO NOT RETURN YOUR FORM TO THE ABOVE ADDRESS.					
1. REPORT DATE (DD-MM-YYYY) 10-Jun-2011		2. REPORT TYPE Technical Paper (Public Release)		3. DATES COVERED (From - To)	
4. TITLE AND SUBTITLE SPACE-TIME CODING FOR AERONAUTICAL TELEMETRY: PART II – EXPERIMENTAL RESULTS				5a. CONTRACT NUMBER	
				5b. GRANT NUMBER	
				5c. PROGRAM ELEMENT NUMBER	
6. AUTHOR(S) Michael Rice, Brigham Young University, Provo, UT Kip Temple, Air Force Flight Test Center, Edwards AFB, CA				5d. PROJECT NUMBER	
				5e. TASK NUMBER	
				5f. WORK UNIT NUMBER	
7. PERFORMING ORGANIZATION NAME(S) AND ADDRESS(ES) AND ADDRESS(ES) 412 TENG/ENI 307 E. Popson Ave. Edwards AFB, CA, 93523				8. PERFORMING ORGANIZATION REPORT NUMBER AFFTC-PA-11139	
9. SPONSORING / MONITORING AGENCY NAME(S) AND ADDRESS(ES) 812 TSS/ENT 307 E. Popson Ave. Edwards AFB, CA, 93523				10. SPONSOR/MONITOR'S ACRONYM(S) N/A	
				11. SPONSOR/MONITOR'S REPORT NUMBER(S)	
12. DISTRIBUTION / AVAILABILITY STATEMENT Approved for public release A: distribution is unlimited.					
13. SUPPLEMENTARY NOTES CA: Air Force Flight Test Center Edwards AFB CA CC: 012100					
14. ABSTRACT Experiments involving side-by-side comparisons of traditional two-antenna transmissions and space-time coded (STC) transmissions involving two transmit antennas confirm theoretical predictions that space time coding is effective in removing signal dropouts caused by the “two-antenna problem.” The experiments involved real transmitters on an airborne platform and a prototype demodulator operating at the Air Force Flight Test Center. The theory is confirmed both by the behaviors of the received signal powers from the two signaling approaches as well as the improved link availability based on the bit error rate performance.					
15. SUBJECT TERMS Space Time Coding, Telemetry, test article antennas, co-channel interference, antenna nulls					
16. SECURITY CLASSIFICATION OF: Unclassified			17. LIMITATION OF ABSTRACT None	18. NUMBER OF PAGES 16	19a. NAME OF RESPONSIBLE PERSON 412 TENG/EN (Tech Pubs)
a. REPORT Unclassified	b. ABSTRACT Unclassified	c. THIS PAGE Unclassified			19b. TELEPHONE NUMBER (include area code) 661-277-8615

SPACE-TIME CODING FOR AERONAUTICAL TELEMETRY: PART II – EXPERIMENTAL RESULTS

Michael Rice
Brigham Young University
Provo, Utah, USA

Kip Temple
Air Force Flight Test Center
Edwards AFB, California, USA

ABSTRACT

Experiments involving side-by-side comparisons of traditional two-antenna transmissions and space-time coded (STC) transmissions involving two transmit antennas confirm theoretical predictions that space time coding is effective in removing signal dropouts caused by the “two-antenna problem.” The experiments involved real transmitters on an airborne platform and a prototype demodulator operating at the Air Force Flight Test Center. The theory is confirmed both by the behaviors of the received signal powers from the two signaling approaches as well as the improved link availability based on the bit error rate performance.

INTRODUCTION

Theoretical analyses over the past seven years have shown that transmit diversity, in the form of space-time coding, solves the “two antenna problem” [1] – [3]. However, it has only been within the last year that flight test experiments have tested this theory. In October 2010, flight tests were conducted at the Air Force Flight Test Center to see if the theoretical promise of space-time coding carries over to operational environments using real hardware. These test involved an air-worthy space-time coded SOQPSK transmitter and a prototype demodulator described in the companion paper [4] operating at a data rate of 10 Mbits/s. This paper presents the results of these tests and shows that space-time coding is effective in eliminating the signal outages caused by the “two-antenna problem.”

TEST CONFIGURATION

The airborne system was designed to simultaneously produce space-time coded and traditional two-antenna transmissions using SOQPSK-TG. This approach eliminated aircraft location and antenna placement as variables in the comparison. The test signaling parameters are summarized in the table below.

Parameter	STC Link	Reference Link
Data	length-4095 PN	length-4095 PN
Data Rate	10 Mbits/s	10 Mbits/s
Over-the-air Data Rate	10.4 Mbits/s	10 Mbits/s
Modulation	SOQPSK-TG	SOQPSK-TG
Carrier Frequency	1485.5 MHz	1514.5 MHz
Power per transmit antenna	5 W	5 W

The over-the-air data rate for STC link is higher than the data rate because of pilot bit insertion. The pilot bits are required to estimate the channel gains between each transmit antenna and the receive antenna as described in [4].

The test parameters do not eliminate carrier frequency as a variable because the two transmissions were assigned to different L-band carrier frequencies. The side-by-side comparison is still meaningful because the wavelengths of the reference link and STC link carriers, 20.20 cm and 19.81 cm, respectively, are not that different. One way of visualizing the impact of the wavelength difference is to compute the *composite* radiation pattern for two antennas whose positions are the same as those used in the test flights (see Figure 3). Assuming the antennas are perfect isotropic radiators and neglecting any influence from the aircraft or cable length differences between the antennas, idealized versions of the composite radiation patterns are easily computed. A plot of the azimuth cut (or aircraft yaw plane) of the idealized radiation patterns at the two carrier frequencies are shown in Figure 1. Both patterns exhibit lobing, especially at azimuth angles corresponding to broadside propagation. The energy radiated from the front or rear of the aircraft is either very high or very low. The key feature here is how similar the two patterns are. Consequently, observations regarding link performance at one frequency apply at the other. The reader should bear in mind that the radiation patterns of Figure 1 apply only to the case where the same signal is applied to both antennas (that is, the traditional approach represented by the reference signal) – the radiation pattern for space-time coded transmission is quite different.

The system used to generate the STC and reference signals is illustrated in Figure 2. The STC transmitter produces a pair of 10 W space-time coded SOQPSK-TG waveforms. These signals are applied to isolators, attenuated to 5 W, and combined with the reference link signals. The reference link signals are produced using a traditional 10 W SOQPSK-TG modulator. The modulator output is split and applied to the combiners as shown. Power levels between the STC and reference links are matched so as not to give a link margin advantage to either signal. Because carrier frequencies are close, cable losses to the antennas can be assumed to be the same. The output of one combiner is connected to the antenna on the top of the fuselage; the output of the other combiner is applied to the antenna on the bottom of the fuselage. The exact antenna locations are illustrated in Figure 3.

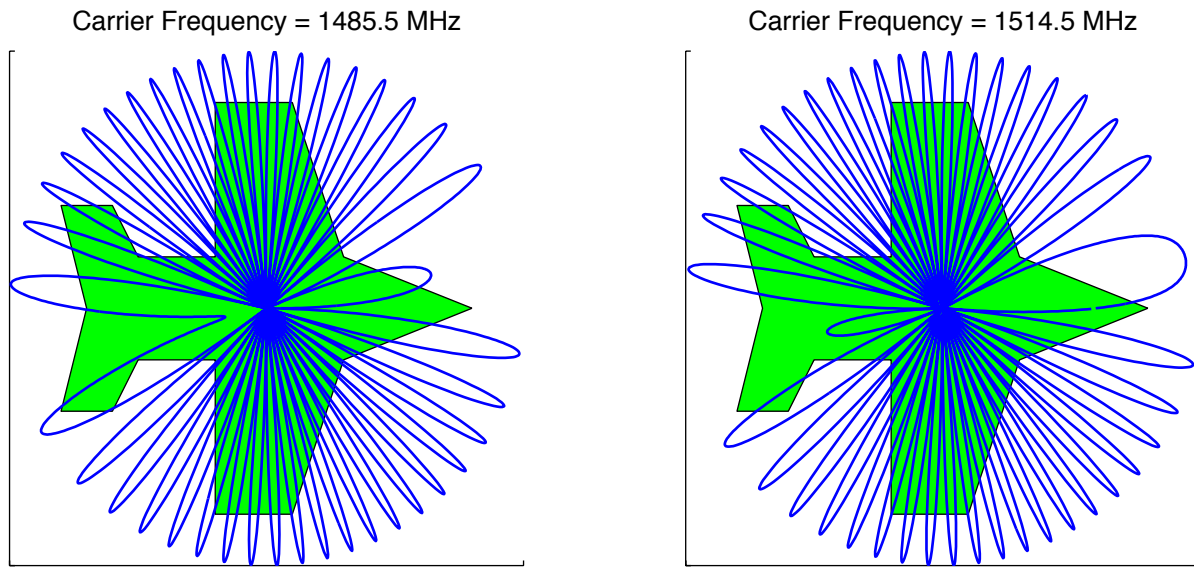


Figure 1: Idealized conceptions of the composite radiation pattern for the two frequencies used in the tests. Note that these radiation patterns only apply to Reference Link (simultaneous transmission of the same signal from both antennas).

Also shown in Figure 2 is another SOQPSK transmitter used for a 1 Mbit/s housekeeping link containing GPS and AHRS data. This data was used to correlate the bit error rate and received signal strength data (recorded at the ground station) with the aircraft location. The housekeeping link was assigned to 1496.5 MHz and used a separate antenna on bottom of the fuselage.

The ground station was located at Building 4795 within the AFFTC complex. The arrangement used is illustrated in Figure 4. The receive antenna was a 5-meter parabolic reflector that tracked the housekeeping link. Three multicoupler outputs from the right hand circularly polarized (RHCP) antenna feed were used. The telemetry receiver/demodulator used one output. Another output was connected to a spectrum analyzer for monitoring the test. The remaining output was split into 4 signals using the 1-to-4 splitter shown. Two of the outputs were applied to receivers tuned to the Reference Link frequency of 1514.5 MHz. The two remaining outputs were applied to receivers tuned to the STC frequency of 1485.5 MHz. In each case, one receiver was used to perform RF to IF conversion prior to demodulation and the second receiver was used to track the received signal strength (measured using the AGC voltage).

The outputs of both demodulators were applied to Fireberd 6000A bit error rate test sets. The number of bit errors and number of severely errored seconds (SES) [6] were recorded and used to assess the qualities of the links and formed the basis of the side-by-side comparison.

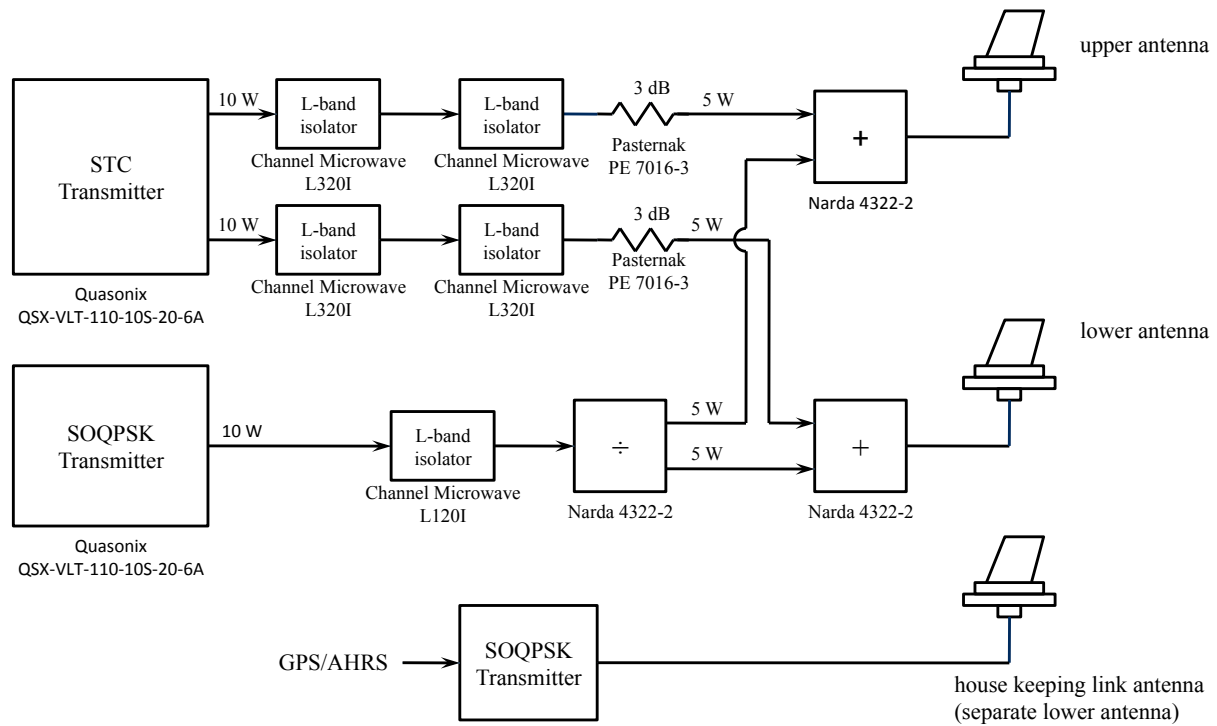


Figure 2: A block diagram of the airborne configuration.

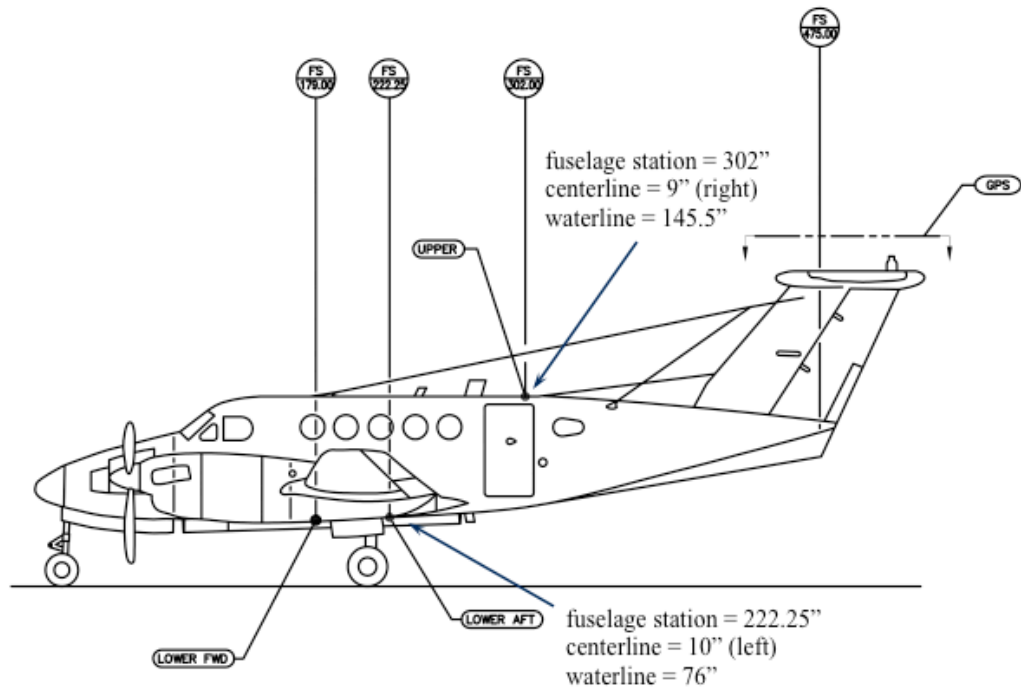


Figure 3: The positions of the two transmit antennas.

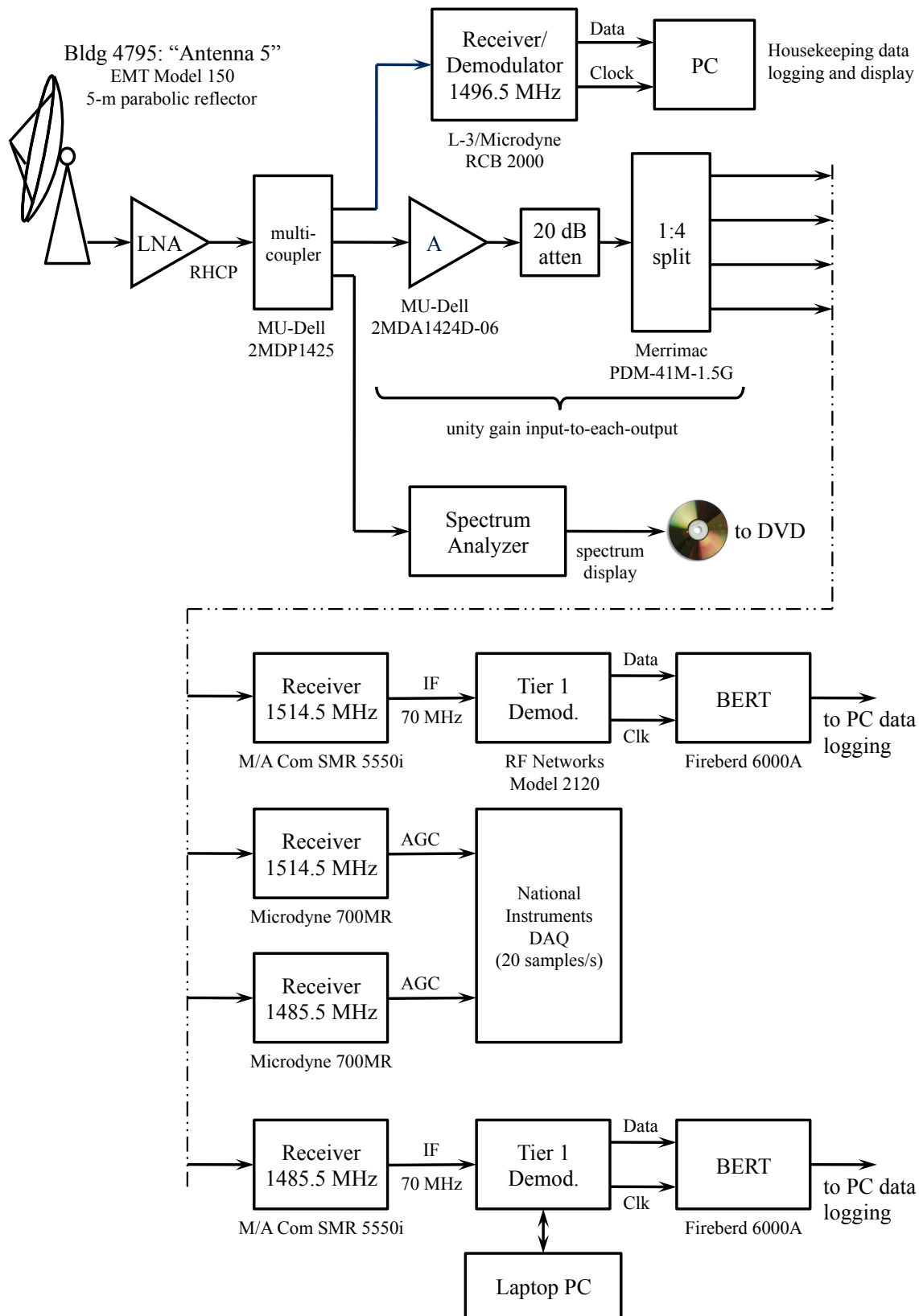


Figure 4: A block diagram of the ground station configuration.

Six test points were defined for flight test. Two of the test points were circles at a 10° bank (points M1/M2) and two were circles at 30° bank (points M3/M4). The intent of these flight paths was to examine link performance through a 360° “cut” through the composite radiation pattern formed by the two antennas using traditional signaling. (See Figure 1 and the accompanying discussion earlier in this section.) The 10° bank and the 30° bank gave different elevation angle “cuts” in azimuth. The last two test points were along the Cords Road flight corridor (points C2/D2). The C-12 performed alternating 30° bank turns off centerline to form a series of “S-turns” along the route. The intent of these test points was twofold. One, assess the performance of the STC link at low signal-to-noise ratio, which occurred when the aircraft was at the east end of the Cords Road corridor, and two, compare link performance as the ground station antenna encountered aircraft antenna pattern nulling created as the aircraft performed the S-turns down the flight path. The entire flight path is plotted in

TEST RESULTS

The side-by-side comparison is based on the link availability achieved by each of the approaches. The *link availability* (LA) is defined by [6]

$$LA = \frac{T_{TOTAL} - T_{SES} - T_{LT}}{T_{TOTAL}} \quad (1)$$

where

T_{TOTAL} = the measurement interval (seconds).

T_{SES} = the number of severely errored seconds. A severely errored second is a one second interval in which the number of bit errors equals or exceeds the equivalent of a 10^{-3} bit error rate if the same error occurrence rate were to occur on an average basis.

T_{LT} = the “lost time” during the measurement interval. In non-precise terms, “lost time” occurs when the bit error rate test set loses synchronization. Most often, synchronization loss is the result of a large number of errors in a very short time. (Bit error rate test sets do not count loss of synchronization as a severely errored second.)

Usually LA is expressed as a percentage. LA is a commonly used metric for link quality in aeronautical telemetry [7]—[11]. The link availabilities for the six test points are summarized in the table below. In all cases, the link availability for the STC link was greater than that of the reference link. The most dramatic improvements occurred at test points M1, M3, and C2. Due to space limitations, points M1, M3 and the M3-to-C2 transition are examined in detail below.

Test Point	Description	Duration	Reference Link			STC Link		
			SES	Bit Errors	LA	SES	Bit Errors	LA
M1	left-hand turn, 10° bank	00:06:30	33	40203753	91.5%	0	47	100.0%
M2	right-hand turn, 10° bank	00:05:20	9	13598222	97.2%	5	6032124	98.4%
M3	left-hand turn, 30° bank	00:01:10	9	9237789	93.1%	1	199242	99.2%
M4	right-hand turn, 30° bank	00:02:00	5	5230738	95.8%	4	46536	96.7%
C2	Cords Road W-E, 30° S-turns	00:17:20	157	48175682	84.9%	38	11311520	96.3%
D2	Cords Road E-W, 30° S-turns	00:17:20	131	239462831	87.4%	102	41716052	90.2%

A plot of the flight path for test point M1 (left-hand turn) is plotted in Figure 6. The corresponding IF signal-to-noise ratio (SNR) and cumulated bit errors are plotted in Figure 7. During the turn, the air-to-ground link looks through front, right-hand side, rear, and left-hand side of the aircraft.

- At the beginning of the test point, the aircraft heading is 180° so that the C-12 is facing the receive antenna. Consequently, propagation is through the front of the aircraft.
- As the aircraft executes the turn, a broadside view of the aircraft is presented to the ground station. This view occurs from approximately 15:48:00 to 15:49:30. The received signal is from the right-hand side of the C-12; and because of the left-hand turn, the lower antenna is in clear view and the upper antenna is partially obscured. The received power variations on the Reference Link are characteristic of severe lobes in the composite radiation pattern as described in the previous section in conjunction with Figure 1. Note the absence of this phenomenon in the received power on the STC link.
- As the turn continues, propagation through the rear of the aircraft is presented to the ground station. This occurs from 15:49:30 to 15:50:00. Both the Reference Link and the STC Link show a marked drop in received power. Evidently, neither antenna produces as much radiated power to the rear of the aircraft.
- Finally, from 15:50:00 to 15:52:00, the broadside view from the left-hand side of the C-12 is now presented to the ground station. Here, the bottom antenna is partially obstructed by the fuselage and the clearest path of from the top antenna. As with the broadside view from the other side of the aircraft, the received Reference Link

power shows variations characteristic of lobes in the composite radiation pattern. And again, this phenomenon is not present in the STC Link.

Most of the variations in received power on the Reference Link are due to the lobing caused by simultaneous transmission from the upper and lower antennas. Figure 1 predicts such power fluctuations for flight paths that change the azimuth presented to the ground-based receiver. Given the simplifications used to produce Figure 1, it is remarkable how well Figure 1 matches the experimental measurements.

Curiously, the dramatic performance advantage of the STC Link over the Reference Link was not repeated when the C-12 flew a right-hand turn with the same bank angle in the same airspace. The flight path and link performance results for this scenario, labeled test point M2, are plotted in Figure 8 and Figure 9. For reasons that are not entirely clear, the received power on the STC link is approximately 10 dB below the Reference Link power.¹ Consequently, any bit error rate advantages realized by space-time coding are muted by the link margin reduction. In any event, the received Reference Link power shows variations characteristic of lobing in the composite antenna gain pattern whereas the received STC Link power shows no such variations. We conclude that at this test point, space-time coding is able to solve the “two-antenna problem” but the link availability improvement is small because of the difference in received signal-to-noise ratio.

Test point M3 is similar to test point M1, except the bank angle was increased to 30°. This flight profile provides another “slice” through the C-12 transmit antenna gain pattern(s). The flight path is plotted in Figure 10 and the experimental results are plotted in Figure 11. At the start of the test point, the C-12 is facing the ground station. About half way through the test point, the receive antenna is “looking” through the rear of the C-12. The Reference Link fails completely at this point due to self-interference caused by the “two antenna problem” as predicted by Figure 1. The severe drop in received signal power marks this point at approximately 16:08:10. The STC Link also experiences a drop in received power (reduced signal power from the rear of the C-12 is a consistent characteristic of this antenna configuration at L-band). However, because space-time coding also removes the self-interference, a large number of bit errors do not occur.

Another interesting data point is the transition from test point M3 to test point C2. The flight path is illustrated in Figure 12. This flight profile presents a lengthy period of broadside propagation from the C-12. Recall from Figure 1 that idealized composite beam pattern exhibits most of the lobing from broadside views of the aircraft. The received power and bit error results for this flight segment are plotted in Figure 13. The received power for the reference link shows variations typical of the lobing predicted by Figure 1. The corresponding impact on the bit error performance is also shown. Observe that the received power on the STC link does not show variations due to lobing.

¹ This phenomenon is also observed with test point M4, a right-hand turn at a 30 bank angle. Evidently, these slices through the antenna radiation pattern do not produce as much power as the slices created by left-hand turns.

CONCLUSIONS

The experiments described in this paper confirm that space-time coding, operating in a real environment, eliminate link outages caused by the “two antenna problem.” This conclusion is supported both by the behavior of the received signal power on the two links and by the improved link availability measured during the tests.

ACKNOWLEDGEMENTS

The authors acknowledge the hard work and contributions of Mr. Glen Wolf (Delphi Research, Inc., Air Force Flight Test Center) who put the system together and the pilots of the C-12 aircraft.

This work was supported by the Test Resource Management Center (TRMC) Test and Evaluation Science and Technology (T&E/S&T) Program through a grant to BYU from the US Air Force Flight Test Center under contract FA9302-05-C-0001 and from the U.S. Army Program Executive Office for Simulation, Training, and Instrumentation (PEO STRI) under contract W900KK-09-C-0016.

REFERENCES

- [1] M. Jensen, M. Rice, and A. Anderson, “Aeronautical Telemetry Using Multiple-Antenna Transmitters,” IEEE Transactions on Aerospace and Electronic Systems, vol. 43, no. 1, pp. 262 – 272, January 2007.
- [2] T. Nelson, M. Rice, and M. Jensen, “Experimental Results with Space-Time Coding Using FQPSK,” in Proceedings of the International Telemetry Conference, Las Vegas, NV, October 2005.
- [3] M. Jensen, M. Rice, T. Nelson, and A. Anderson, “Orthogonal Dual-Antenna Transmit Diversity for SOQPSK in Aeronautical Telemetry Channels,” in Proceedings of the International Telemetry Conference, San Diego, CA, October 2004.
- [4] M. Rice, “Space-Time Coding for Aeronautical Telemetry: Part I – System Description,” in Proceedings of the International Telemetry Conference, Las Vegas, NV, October 2011.
- [5] IRIG 106-09: Telemetry Standards. Range Commanders Council Telemetry Group, Range Commanders Council, White Sands Missile Range, NM.
- [6] R. Jefferis, “Link Availability and Error Clusters in Aeronautical Telemetry,” in Proceedings of the International Telemetry Conference, Las Vegas, NV, October 1999.
- [7] K. Temple, “ARTM Tier II Waveform Performance,” in Proceedings of the International Telemetry Conference, Las Vegas, NV, October 2003.

- [8] R. Jefferis, "Telemetry Link Reliability Improvement Via "No-Hit" Diversity Branch Selection," in Proceedings of the International Telemetry Conference, San Diego, CA, October 2004.
- [9] K. Temple, "Performance Trade-Offs When Implementing Turbo Product Code Forward Error Correction for Airborne Telemetry," in Proceedings of the International Telemetry Conference, Las Vegas, NV, October 2005.
- [10] K. Temple, R. Jefferis, and R. Selbrede, "Performance Characterization of Multi-Band Antennas for Aeronautical Telemetry," in Proceedings of the International Telemetry Conference, Las Vegas, NV, October 2007.
- [11] K. Temple and R. Selbrede, "Performance Comparison of Aeronautical Telemetry in S-Band and C-Band," in Proceedings of the International Telemetry Conference, San Diego, CA, October 2010.



Figure 5: The entire flight path for the STC tests. The individual test points are plotted in the figures that follow.



Figure 6: Test point M1 – a left-hand turn at a 10° bank. The flight path is the circle near the top of the image. The receiving site is the circle inside the shaded area.

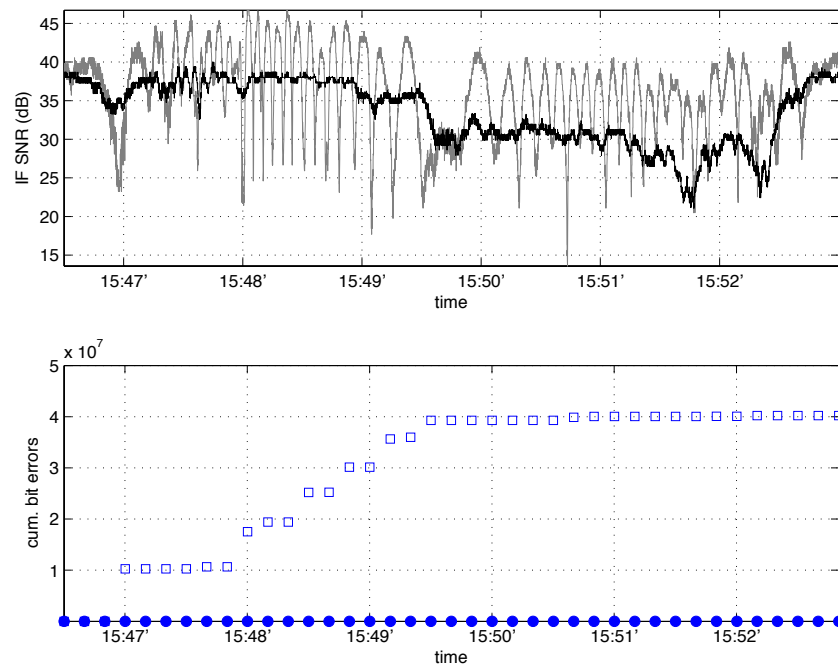


Figure 7: Results for test point M1. Top: the IF SNR for the reference link (gray line) and the STC link (dark heavy line). Bottom: the cumulated bit errors measured during the test point for the reference link (squares) and the STC link (filled circles).



Figure 8: Test point M2 – a right-hand turn at a 10° bank. The flight path is the circle near the top of the image. The receiving site is the circle inside the shaded area.

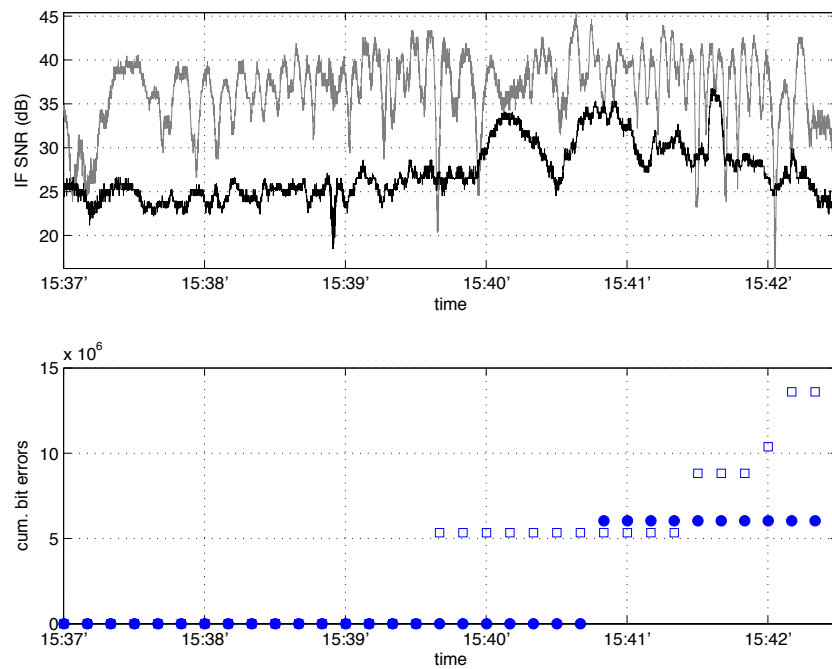


Figure 9: Results for test point M2. Top: the IF SNR for the reference link (gray line) and the STC link (dark heavy line). Bottom: the cumulated bit errors measured during the test point for the reference link (squares) and the STC link (filled circles).



Figure 10: The flight path for test point M3 – a left-hand turn at a 30° bank. The flight path is the circle near the top of the image. The receiving site is the circle inside the shaded area.

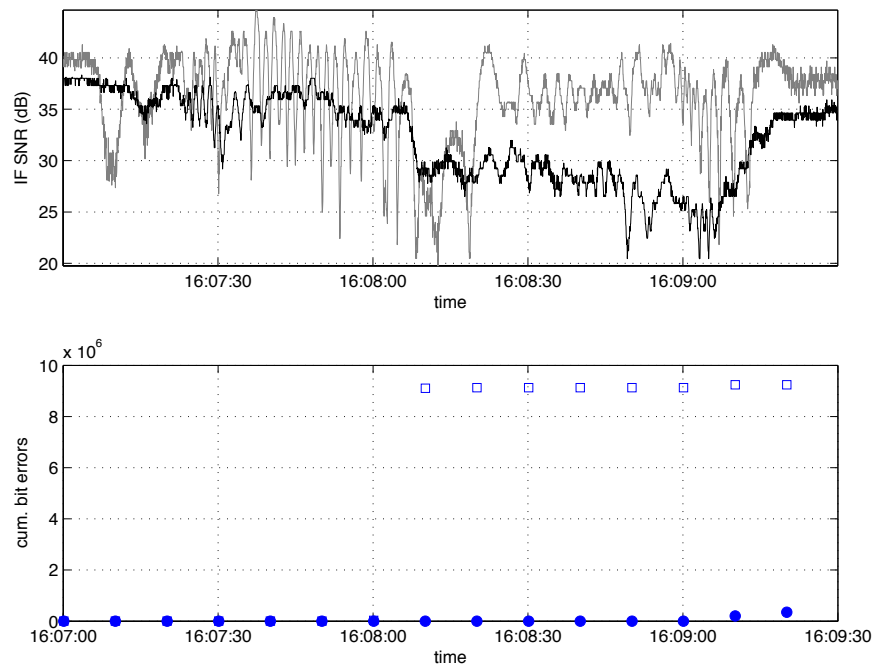


Figure 11: Results for test point M3. Top: the IF SNR for the reference link (gray line) and the STC link (dark heavy line). Bottom: the cumulated bit errors measured during the test point for the reference link (squares) and the STC link (filled circles).

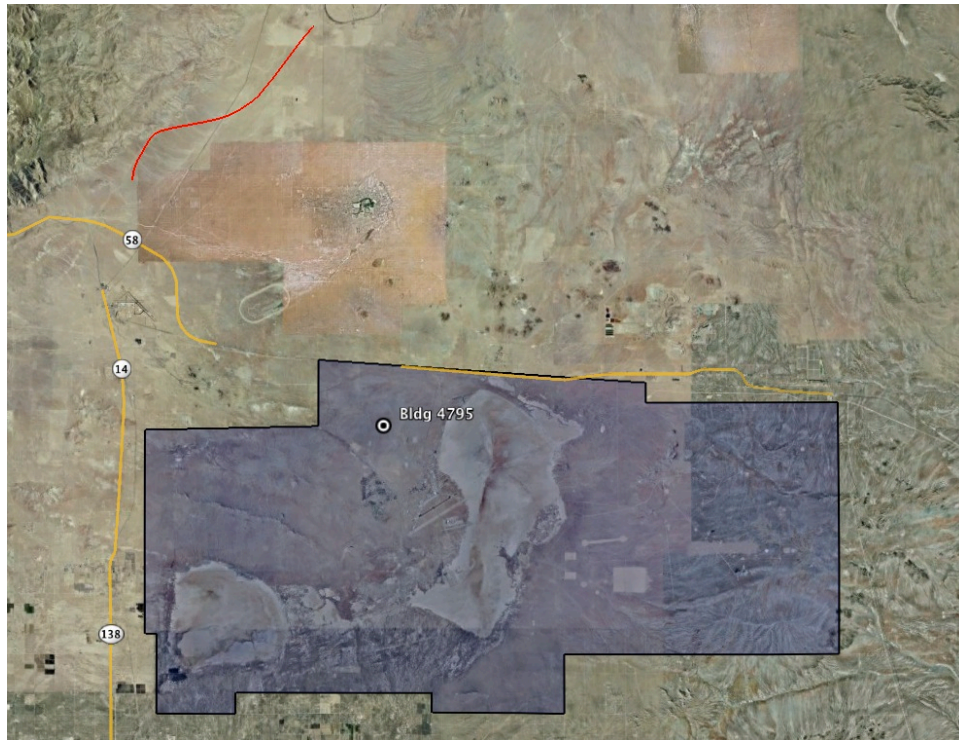


Figure 12: The flight path for test point M3-to-C1 transition. The flight path is the “dog leg” path near the upper left corner of the image. The receiving site is the circle inside the shaded area.

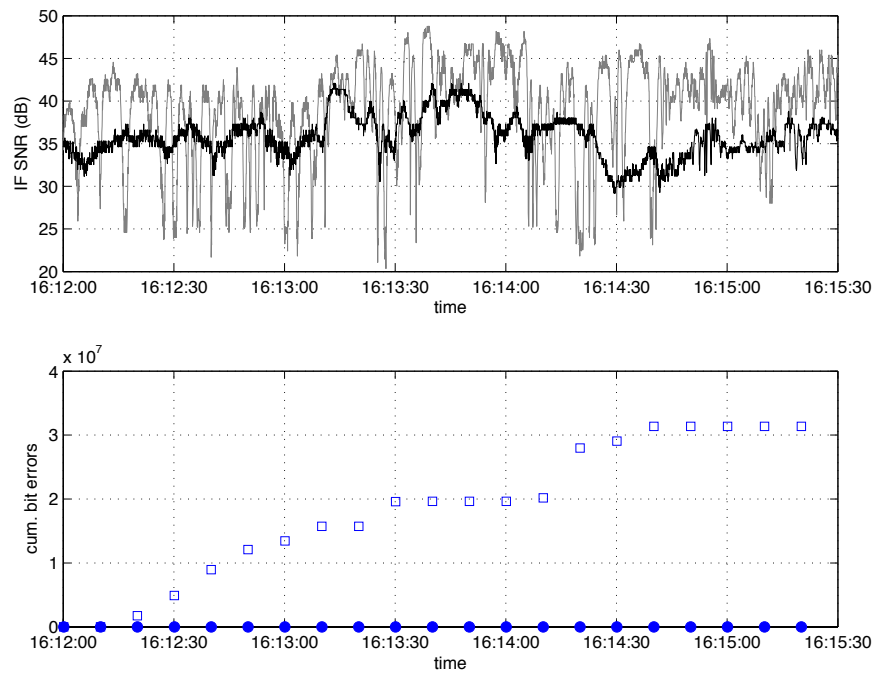


Figure 13: Results for test point M3-to-C1 transition. Top: the IF SNR for the reference link (gray line) and the STC link (dark heavy line). Bottom: the cumulated bit errors measured during the test point for the reference link (squares) and the STC link (filled circles).